Advanced Powder Technology xxx (xxxx) xxx

Contents lists available at ScienceDirect

Advanced Powder Technology

journal homepage: www.elsevier.com/locate/apt

Original Research Paper

Ion reduction in iron oxide and oxyhydroxide nanoparticles during ultrasonic treatment

S.V. Stolyar [a,b], O.A. Bayukov [b], R.N. Yaroslavtsev [a,b], Yu.V. Knyazev [b], V.P. Ladygina [c], Yu.V. Gerasimova [b], R.S. Iskhakov [b]

[a] Siberian Federal University, Krasnoyarsk, Russia
[b] Kirensky Institute of Physics, Federal Research Center KSC SB RAS, Krasnoyarsk, Russia
[c] Krasnoyarsk Scientific Center, Federal Research Center KSC SB RAS, Krasnoyarsk, Russia

ARTICLE INFO

Article history:
Received 19 November 2018
Received in revised form 4 March 2019
Accepted 5 August 2019
Available online xxxx

Keywords:
Nanoparticles
Ferrihydrite
Ultrasonic cavitation

ABSTRACT

The effect of ultrasonic treatment of iron oxide and iron oxyhydroxide nanoparticles (ferrihydrite nanoparticles synthesized by *Klebsiella oxytoca* microorganisms, ferrihydrite nanoparticles synthesized by a chemical method and hematite nanoparticles) is studied. Samples of nanoparticles were investigated using transmission electron microscopy, Mössbauer spectroscopy and X-ray diffraction methods. The formation of the α-Fe metal phase from nanoparticles of iron oxides and iron oxyhydroxides was detected. The metal phase is formed as a result of the reduction of iron ions during cavitation treatment. According to the experimental results, the presence of a protein or a polysaccharide component is necessary for the course of this reaction.

1. Introduction

Ultrasound is used in various fields such as medicine, microbiology, chemical and bioleaching, synthesis of new compounds, etc [1]. Sonochemical synthesis is a promising method for the preparation of nanomaterials with unique properties, due to the extreme conditions achieved in the process of ultrasonic cavitation [2,3]. Acoustic and thermal effects of cavitation, in particular, contribute to the thermolysis of water molecules with the appearance of free hydrogen bonds [4]. As a result of subsequent reactions, various free radicals are formed, including those with reducing properties. The latter opens up opportunities for the realization of chemical reactions and the synthesis of new compounds [3,5]. The formation of metallic noble metal nanoparticles in solutions of their salts during the ultrasonic treatment in the cavitation regime does not require a chemical reducing agent and proceeds at a tremendous rate [2]. The reduction of 3d metal ions was reported in [6], in which it was shown that ultrasonic treatment in the cavitation regime leads to the reduction of divalent copper oxide in the glycerol solution to monovalent copper oxide.

In this study, we investigated the effect of ultrasonic treatment in the cavitation regime on the magnetic nanoparticles of iron oxide and oxyhydroxide. We used ferrihydrite nanoparticles synthesized by *Klebsiella oxytoca* microorganisms, ferrihydrite nanoparticles synthesized by a chemical method and hematite nanoparticles.

Microorganisms are well known in microbiology and geochemistry, due to their ability to mineralize large amounts of iron under anaerobic conditions, in particular, synthesizing and storing ferrihydrite [7,8]. One such microorganism is *Klebsiella oxytoca*, which synthesizes biogenic polysaccharide-ferrihydrite nanoparticles, known as Fe(III)-exopolysaccharide (Fe-EPS) [7,9]. Ferrihydrite ($5Fe_2O_3{\cdot}9H_2O$) is a metastable form of iron oxyhydroxide and a precursor of such minerals as hematite and goethite [10]. The importance of ferrihydrite for the iron circulation in the environment and metallurgical processes attract much attention of the scientific community for a long time [7,11,12]. Ferrihydrite is an antiferromagnetic compound (T_N = 350 K) [13], but, in the nanodispersed form, it turns out to be ferrimagnetic state due to decompensation of the magnetic moments of Fe^{3+} ions on the surface and in the volume of particles. The magnetic susceptibility of ferrihydrite particles, enhanced by the superantiferromagnetism effect, provides ample opportunities for magnetic control of these objects [14–16], which opens the way for their use in nanomedicine and biotechnology.

E-mail address: yar-man@bk.ru (R.N. Yaroslavtsev)

https://doi.org/10.1016/j.apt.2019.08.009
0921-8831/

2. Experimental

All the chemicals used in this work were of analytical grade and used without further purification. Hematite nanoparticles (α-Fe_2O_3) were synthesized by chemical deposition from a solution. Synthesis of nanoparticles was carried out at room temperature and constant stirring by dropwise adding an aqueous solution of ammonia (15 vol%) to an aqueous solution of iron (III) chloride (1 wt%). The precipitate was washed with distilled water.

Synthetic ferrihydrite was synthesized by slow addition of an alkaline NaOH solution (1 M) to a solution of ferric chloride $FeCl_3$ (0.02 M) at room temperature with constant stirring until the pH reached a neutral value [17].

We used the biomass of *Klebsiella oxytoca* microorganisms, which were cultivated for 7–14 days to obtain ferrihydrite nanoparticles [18]. Bacterial biomass was separated from the supernatant by centrifugation to separate the ferrihydrite and produce the sol. The resulting precipitate was incubated in acetone for 30 min to remove the fatty acids, washed with distilled water and then sonicated. The resulting precipitate was washed with distilled water with the addition of NaCl to a neutral pH supernatant and again sonicated in cavitation mode.

The ultrasonic treatment in the cavitation regime of the synthesized samples was carried out in a Volna UZTA-0.4/22-OM setup (22 kHz, 50 W/cm^2).

The nanoparticle samples were examined with a Hitachi HT7700 transmission electron microscope (accelerating voltage 100 kV) of the Center for Collective Use, Krasnoyarsk Scientific Center, Krasnoyarsk, Russia. Mössbauer spectra were measured on an MC-1104E5m spectrometer with the 57Co(Cr) source at room temperature on powder samples with a thickness of 5–10 mg/cm^2 on the basis of the natural iron content. Isomer chemical shifts are accounted in reference to α-Fe. X-ray diffraction (XRD) patterns were obtained on a diffractometer with Cu(Kα) radiation in a 2-theta range of 20–80°.

3. Results and discussion

3.1. Biogenic ferrihydrite nanoparticles

The FTIR spectrum was obtained and analyzed (Fig. 1) to identify the organic shell covering the ferrihydrite nanoparticles. IR spectra were recorded over the spectral range of 350–4000 cm^{-1} on the samples inserted into the KBr matrix. The inset of Fig. 1 presents the spectrum of this sample in a polyethylene matrix in the spectral region of 200–700 cm^{-1}.

The spectrum has a broad absorption maximum at 3420 cm^{-1} caused by stretching vibrations of the O—H groups, and the large peak width is, in part, due to the O—H surface bonds [19,20]. Bending vibrations of H_2O appear at a frequency of 1630 cm^{-1} [21,22]. Antisymmetric and symmetric C—O vibrations of adsorbed carbonate are observed at 1498 and 1410 cm^{-1}, respectively [21,23].

It is known that the strains of the bacteria Klebsiella oxytoca produce exopolysaccharides [24], which are involved in the binding of iron ions. The authors of [24] determined that the IR biomass spectrum contains modes corresponding to glucose, polysaccharides, and amines of proteins. The infrared spectra of proteins and their degradation products (peptides) are characterized by the presence of two main absorption bands: amide I (1650 cm^{-1}) and amide II (1550 cm^{-1}), due to stretching vibrations of the C=O bond (amide I) and planar deformation vibrations of the NH bond (amide II) [25]. Thus, if both bands are present in the spectra of tested substance, then it can be argued, with a high probability, that there is a polypeptide or protein in the sample. In the spectrum of the sample under study, modes with such frequencies do not appear, or their intensity is too low against an increasing background of this region.

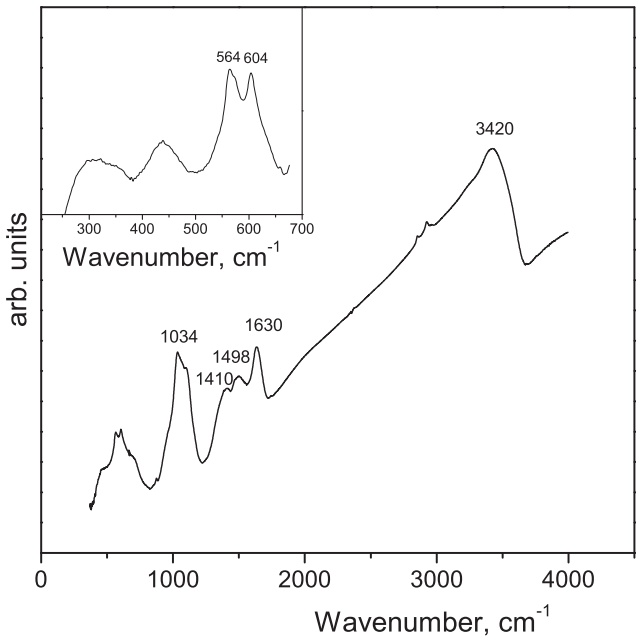

Fig. 1. FTIR spectrum of biogenic ferrihydrite nanoparticles.

The following regions and absorption bands are characteristic of polysaccharides: stretching vibrations of bound OH groups at 3400 cm^{-1}; stretching vibrations of CH groups from 2800 to 3000 cm^{-1}; stretching vibrations of the CH groups of non-ionized and ionized acids at 1740 and 1620 cm^{-1}; latitudinal vibrations of CH groups from 1400 to 1450 cm^{-1}; oscillation bands of the frame of the molecule in the region from 1000 to 1100 cm^{-1}. Analysis of the infrared spectrum of the sample showed a rather large coincidence of the characteristic absorption bands. However, these frequencies can be attributed to the absorption frequencies of ferrihydrite with a minor shift in frequency, and it is possible that this shift determines the presence of the polysaccharide.

The absorption spectrum in the region of fewer than 1300 cm^{-1} is an individual characteristic of the compound; therefore, it is called the "fingerprint" area and pay special attention to it when determining the substance. Complicated band (doublet) in the region of 1100 cm^{-1} may be attributed to the stretching vibrations of the Fe—OH bonds. In the region below 700 cm^{-1}, there are modes 603, 564, 448, 304 cm^{-1} (see inset in Fig. 1), which we attribute to bending O—Fe—O vibrations, Fe—O stretching modes for octahedral and tetrahedral iron cations [26]. Thus, the IR spectroscopy method has shown that nanoparticles of biogenic ferrihydrite are embedded in iron-binding exopolysaccharides.

Fig. 2 shows the results of transmission electron microscopy of two samples. Fig. 2(a) shows the image of the ferrihydrite nanoparticles sample. The average particle size was ~3 nm. Fig. 2(b) shows the image of the sample of ferrihydrite nanoparticles after sonication, on which dense formations (whiskers) with a length of 40 nm and a diameter of 3 nm are observed. The diffraction pattern is characteristic of the so-called 2-line ferrihydrite. [27,28]. Two diffuse reflections with $d_1 = 1.5$ Å and $d_2 = 2.59$ Å interplanar distances are observed.

Fig. 3 shows the Mössbauer spectra obtained at room temperature of the ferrihydrite nanoparticles (curve (a) representing the doublet) and ferrihydrite nanoparticles after sonication (curve (b)). It can be seen that curve (b), in comparison with curve (a), is characterized by an additional sextet. In Table 1, the interpreta-

Please cite this article as: S. V. Stolyar, O. A. Bayukov, R. N. Yaroslavtsev et al., Ion reduction in iron oxide and oxyhydroxide nanoparticles during ultrasonic treatment, Advanced Powder Technology, https://doi.org/10.1016/j.apt.2019.08.009

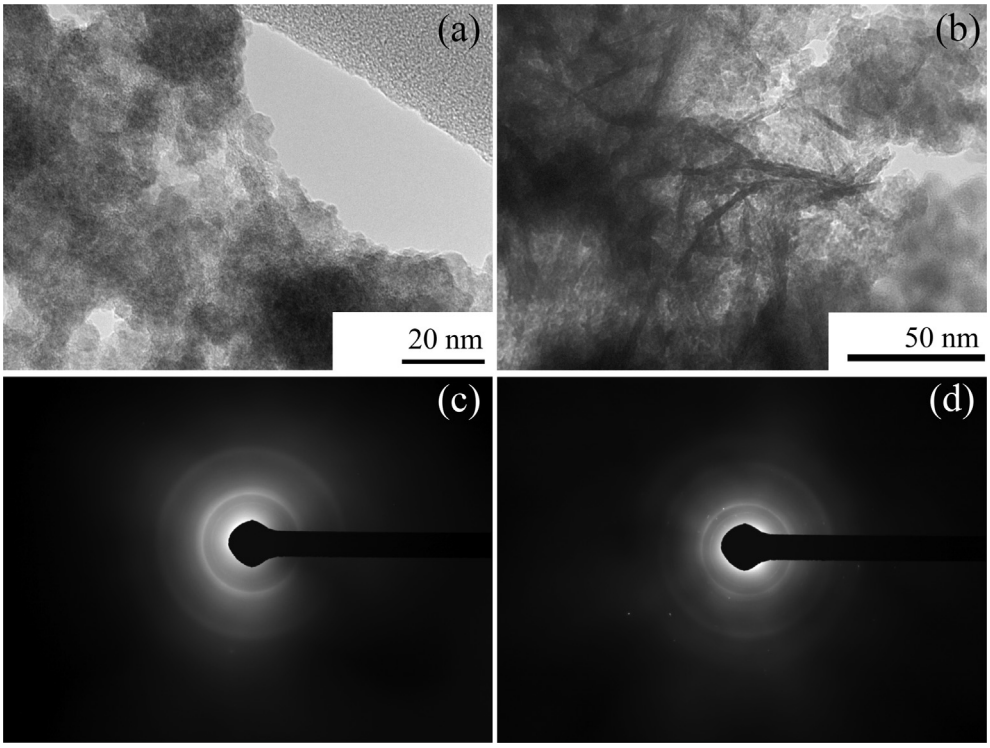

Fig. 2. TEM-images of the biogenic ferrihydrite nanoparticles before sonication (a) and after sonication (b) and microdiffraction patterns of this samples (c, d).

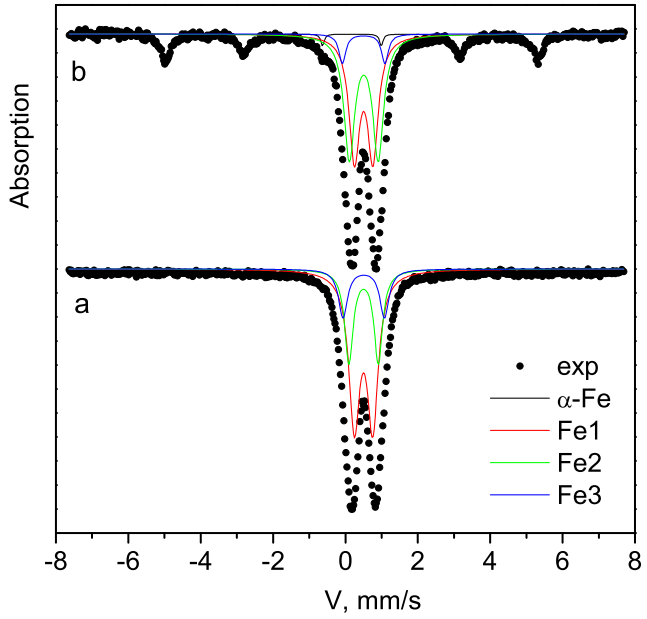

Fig. 3. Mössbauer spectra of the biogenic ferrihydrite nanoparticles before sonication (a) and after sonication (b).

tion of the Mössbauer spectra is given. In the paramagnetic component of (a) and (b) spectra, three main non-equivalent positions of Fe^{3+} ions with octahedral coordination are recorded. These positions can be divided into two groups: positions Fe1 and Fe2 with a relatively small degree of distortion of local symmetry (QS (Fe1) ~ 0.5 mm/s, QS(Fe2) ~ 0.8 mm/s) and positions Fe3 with a high degree of distortion (QS(Fe3) ~ 1–1.5 mm/s). The crystalline structure of ferrihydrite was discussed in [29]. The sextet parameters given in Table 1 indicate the presence of α-Fe metal nanoparticles in the sediment. The Mössbauer sextets recorded at room temperature with α-Fe parameters reveal that the ferromagnetic particle size exceeds 100 Å [30]. The metal component in the sample is equal to 18% (see Table 1).

3.2. Hematite nanoparticles

Ferrihydrite is characterized by the lowest thermodynamic stability among iron oxides and oxyhydroxides. In this part of the work, we investigated the process of ultrasonic treatment of hematite powder in an aqueous medium and in an albumin solution. The use of hematite is due to its thermodynamic stability and known values of magnetic parameters. Since chemically synthesized hematite particles do not have an organic shell, unlike ferrihydrite

Table 1
Mössbauer parameters of biogenic ferrihydrite.

Sample	IS, mm/s	H, kOe	QS, mm/s	W, mm/s	A	Position
(a) Before sonication	0.346	–	0.51	0.37	0.58	Fe1
	0.348	–	0.81	0.29	0.27	Fe2
	0.351	–	1.14	0.30	0.15	Fe3
(b) After sonication	0.024	318	0	0.11	0.18	α-Fe
	0.349	–	0.52	0.35	0.37	Fe1
	0.352	–	0.80	0.36	0.38	Fe2
	0.348	–	1.17	0.22	0.05	Fe3

IS is isomeric shift relative to α-Fe, QS is quadrupole splitting, W is absorption line width, H is hyperfine field at the iron core, and A is iron position occupancy.

Please cite this article as: S. V. Stolyar, O. A. Bayukov, R. N. Yaroslavtsev et al., Ion reduction in iron oxide and oxyhydroxide nanoparticles during ultrasonic treatment, Advanced Powder Technology, https://doi.org/10.1016/j.apt.2019.08.009

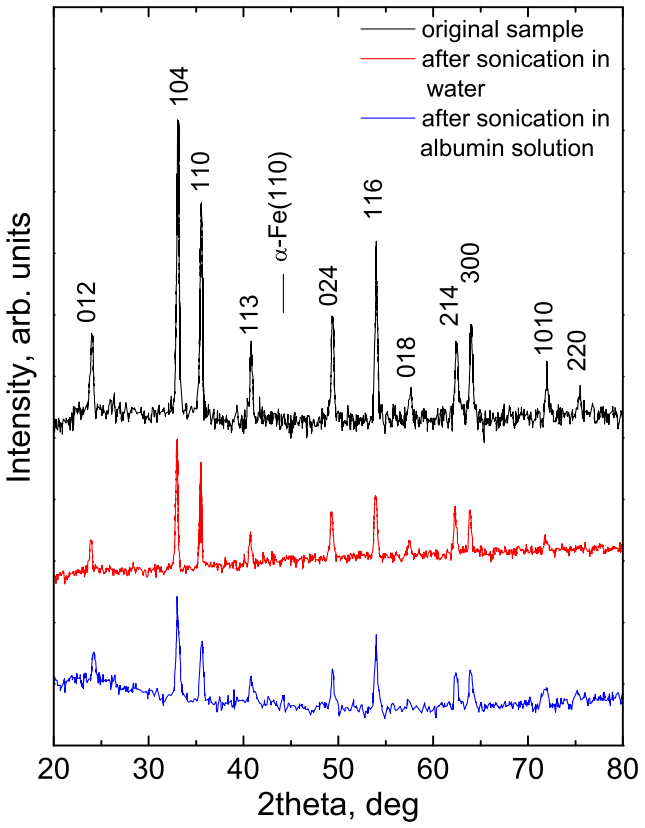

Fig. 4. XRD patterns of hematite samples: before sonication and after sonication in water and in albumin solution.

nanoparticles, in addition to processing in an aqueous medium, the experiment was also carried out in aqueous solution of albumin (2%).

XRD patterns of the original sample and samples subjected to ultrasonic treatment in an aqueous medium and in albumin solution are shown in Fig. 4. All observed reflections in the three samples refer to hematite. After sonication, the lines broaden and its intensity decreases. In the case of a sample subjected to sonication in an albumin solution, a weak reflection near 44.2° is observed which we refer to the α-Fe (1 1 0) reflection.

Fig. 5a and b shows the TEM-image and the microdiffraction pattern of the original hematite powder. The average particle size, according to several images, was 40 nm.

Fig. 5c, d, and e, f show the results of transmission electron microscopy of hematite nanoparticles after sonication in an aqueous medium and in an albumin solution, respectively. The sample sonicated in water is characterized by more diffuse diffraction rings, compared with those of original sample, and higher scatter of nanoparticle sizes. In the case of a sample treated in an albumin solution, the particle sizes become much smaller (~20 nm), and the diffraction pattern is even more diffuse.

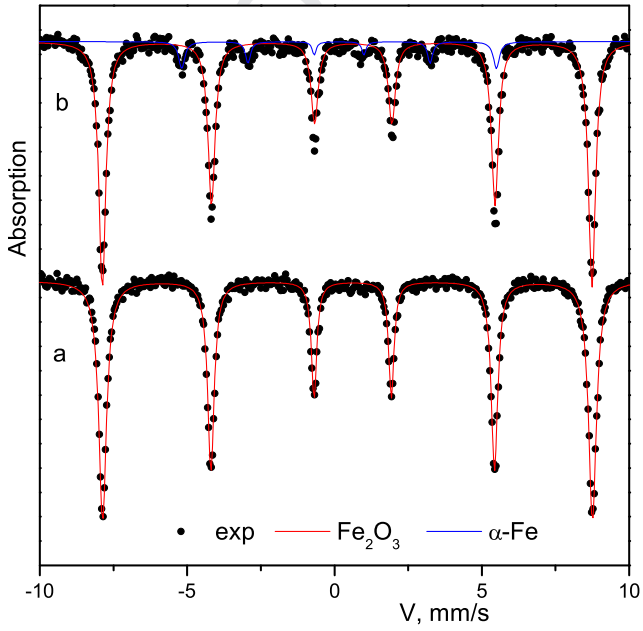

Fig. 6. Mössbauer spectra of the hematite nanoparticles before (a) and after (b) sonication in albumin solution.

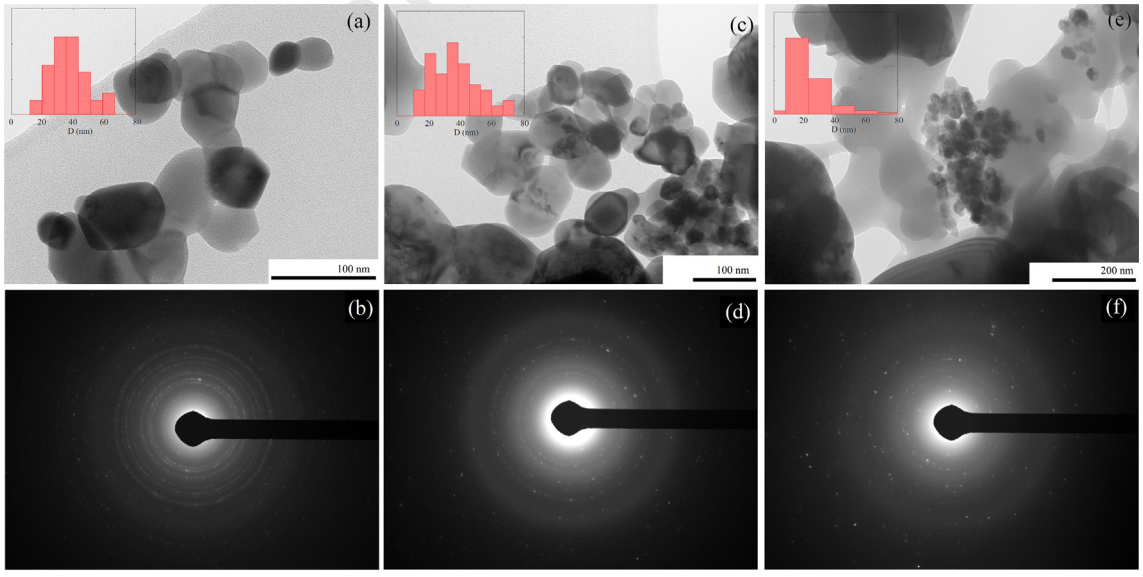

Fig. 5. TEM-images and microdiffraction patterns of hematite nanoparticles. The insets show the particle size distribution. a, b – before sonication; c, d – after sonication in water; e, f – after sonication in albumin solution.

Please cite this article as: S. V. Stolyar, O. A. Bayukov, R. N. Yaroslavtsev et al., Ion reduction in iron oxide and oxyhydroxide nanoparticles during ultrasonic treatment, Advanced Powder Technology, https://doi.org/10.1016/j.apt.2019.08.009

Table 2
Mössbauer parameters of hematite nanoparticles.

Sample	IS, mm/s	H, kOe	QS, mm/s	W, mm/s	A	Position
(a) Before sonication	0.377	517	−0.43	0.27	1.00	α-Fe_2O_3
(b) After sonication in albumin solution	0.380	517	−0.41	0.27	0.93	α-Fe_2O_3
	0	333	0	0.21	0.07	α-Fe

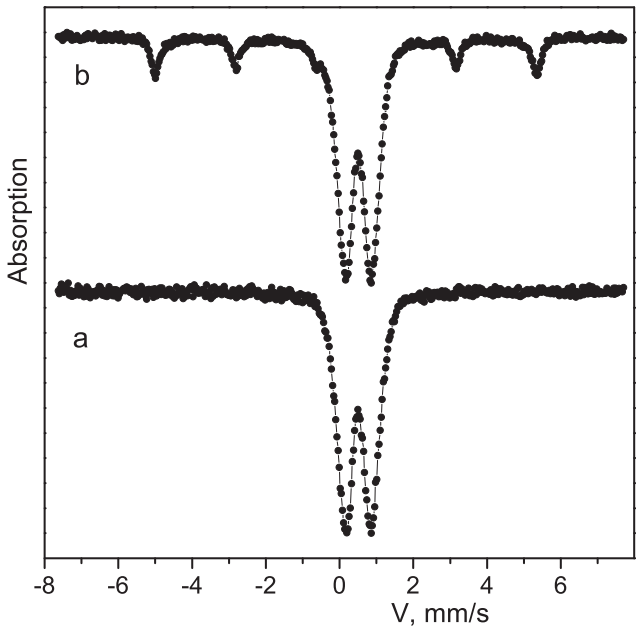

Fig. 7. Mössbauer spectra of the synthetic ferrihydrite nanoparticles before sonication (a) and after sonication in albumin solution (b).

Fig. 6 shows the Mössbauer spectra of hematite nanoparticles measured at T = 300 K. The spectrum of the sample treated with ultrasound in water does not differ from the spectrum of the original sample and it has a sextet characteristic of hematite. The Mössbauer spectrum of the sample sonicated in an albumin solution (Fig. 6b) is characterized by the presence of an additional sextet. The spectrum interpretation (Table 2) showed that the hyperfine structure parameters of the formed phase are characteristic of α-Fe.

3.3. Synthetic ferrihydrite nanoparticles

In addition to studying the effect of ultrasound cavitation on biogenic ferrihydrite nanoparticles, the behavior of synthetic nanoparticles was also carried out. The difference between nanoparticles synthesized by chemical means from biogenic nanoparticles is the absence of an organic shell on the surface. Fig. 7a shows the Mössbauer spectrum of synthetic ferrihydrite nanoparticles, and the results of interpretation are summarized in Table 3. Chemical shift values of Fe^{3+} ions in the case of nanoparticles, obtained by the chemical method are smaller than those of biogenic nanoparticles. This suggests that in the nanoparticles obtained chemically, the number of OH groups surrounding Fe^{3+} ions is less than in the biogenic nanoparticles.

Ultrasonic treatment of synthetic nanoparticles in the aquatic medium did not lead to significant changes in Mössbauer parameters. Fig. 7b shows the Mössbauer spectrum of synthetic ferrihydrite nanoparticles after treatment in the albumin solution. The interpretation results indicate the formation of the α-Fe phase in chemically obtained nanoparticles when treated in the albumin solution, as well as in biogenic nanoparticles. Thus, the formation of the α-Fe phase after ultrasonic treatment of nanoparticles is caused by both cavitational effects and the presence of an organic component (protein or polysaccharide).

4. Conclusion

In this work, we investigated the effects of ultrasonic treatment in the cavitation mode on nanoparticles of iron oxides and oxyhydroxides. The method of infrared spectroscopy was used to identify the organic shell of ferrihydrite nanoparticles synthesized by Klebsiella oxytoca microorganisms. It has been shown that the shell consists of exopolysaccharides. The study of the effect of ultrasonic cavitation on the biogenic ferrihydrite nanoparticles showed that as a result of the treatment, the formation of the metallic phase α-Fe occurs. The reduction of iron ions also occurred by sonication of nanoparticles of synthetic ferrihydrite and hematite with the addition of albumin to the solution. Thus it is determined that this process occurs only in the presence of an organic component (protein or polysaccharide).

Acknowledgements

The reported study was carried out with the financial support of the Russian Foundation for Fundamental Research, the Government of the Krasnoyarsk Territory, the Krasnoyarsk Territory Fund for Support of Scientific and Technical Activity in the framework of scientific Projects No. 18-43-243003 and No. 18-42-243011. The work is supported by the Special Program of the Ministry of Education and Science of the Russian Federation for the Siberian Federal University.

Table 3
Mossbauer parameters of synthetic ferrihydrite nanoparticles.

Sample	IS, mm/s	H, kOe	QS, mm/s	W, mm/s	A	Position
(a) Before sonication	0.351	–	0.51	0.35	0.53	Fe1
	0.355	–	0.86	0.31	0.37	Fe2
	0.359	–	1.21	0.26	0.10	Fe3
(b) After sonication in albumin solution	0.006	332	0	0.25	0.19	α-Fe
	0.350	–	0.53	0.35	0.35	Fe1
	0.351	–	0.84	0.36	0.37	Fe2
	0.357	–	1.22	0.30	0.10	Fe3

Please cite this article as: S. V. Stolyar, O. A. Bayukov, R. N. Yaroslavtsev et al., Ion reduction in iron oxide and oxyhydroxide nanoparticles during ultrasonic treatment, Advanced Powder Technology, https://doi.org/10.1016/j.apt.2019.08.009

References

[1] S. Vyas, Y.-P. Ting, A review of the application of ultrasound in bioleaching and insights from sonication in (Bio)chemical processes, Resources 7 (2017) 3, https://doi.org/10.3390/resources7010003.
[2] J.H. Bang, K.S. Suslick, Applications of ultrasound to the synthesis of nanostructured materials, Adv. Mater. 22 (2010) 1039–1059, https://doi.org/10.1002/adma.200904093.
[3] C. He, L. Liu, Z. Fang, J. Li, J. Guo, J. Wei, Formation and characterization of silver nanoparticles in aqueous solution via ultrasonic irradiation, Ultrason. Sonochem. 21 (2014) 542–548, https://doi.org/10.1016/j.ultsonch.2013.09.003.
[4] M.A. Margulis, Sonoluminescence and sonochemical reactions in cavitation fields. A review, Ultrasonics 23 (1985) 157–169, https://doi.org/10.1016/0041-624X(85)90024-1.
[5] E. Akbay, T.G. Ölmez, Sonochemical synthesis and loading of PbS nanoparticles into mesoporous silica, Mater. Lett. 215 (2018) 263–267, https://doi.org/10.1016/j.matlet.2017.12.117.
[6] R.N. Galiahmetov, A.G. Mustafin, R.R. Garafutdinov, G.M. Kuznetsova, Production of Cu2O nanoparticles under condition of ultrasonically induced cavitation, Lett. Mater. 1 (2011) 176–178, https://doi.org/10.22226/2410-3535-2011-3-176-178.
[7] S. Kianpour, A. Ebrahiminezhad, M. Mohkam, A.M. Tamaddon, A. Dehshahri, R. Heidari, et al., Physicochemical and biological characteristics of the nanostructured polysaccharide-iron hydrogel produced by microorganism Klebsiella oxytoca, J. Basic Microbiol. 57 (2017) 132–140, https://doi.org/10.1002/jobm.201600417.
[8] F. Baldi, A. Minacci, M. Pepi, A. Scozzafava, Gel sequestration of heavy metals by Klebsiella oxytoca isolated from iron mat, FEMS Microbiol. Ecol. 36 (2001) 169–174, https://doi.org/10.1111/j.1574-6941.2001.tb00837.x.
[9] G. Gallo, F. Baldi, G. Renzone, M. Gallo, A. Cordaro, A. Scaloni, et al., Adaptative biochemical pathways and regulatory networks in Klebsiella oxytoca BAS-10 producing a biotechnologically relevant exopolysaccharide during Fe(III)-citrate fermentation, Microb. Cell Fact. 11 (2012) 152, https://doi.org/10.1186/1475-2859-11-152.
[10] J. Majzlan, A. Navrotsky, U. Schwertmann, Thermodynamics of iron oxides: Part III. Enthalpies of formation and stability of ferrihydrite (∼Fe(OH)3), schwertmannite (∼FeO(OH)3/4(SO4)1/8), and ε-Fe2O3, Geochim. Cosmochim. Acta 68 (2004) 1049–1059, https://doi.org/10.1016/S0016-7037(03)00371-5.
[11] C. Rani, S.D. Tiwari, Estimation of particle magnetic moment distribution for antiferromagnetic ferrihydrite nanoparticles, J. Magn. Magn. Mater. 385 (2015) 272–276, https://doi.org/10.1016/j.jmmm.2015.02.048.
[12] O. Strbak, L. Balejcikova, L. Baciak, J. Kovac, M. Masarova-Kozelova, A. Krafcik, et al., Low-field and high-field magnetic resonance contrast imaging of magnetoferritin as a pathological model system of iron accumulation, J. Phys. D. Appl. Phys. 50 (2017), https://doi.org/10.1088/1361-6463/aa8020 365401.
[13] M.S. Seehra, V.S. Babu, A. Manivannan, J.W. Lynn, Neutron scattering and magnetic studies of ferrihydrite nanoparticles, Phys. Rev. B 61 (2000) 3513–3518, https://doi.org/10.1103/PhysRevB.61.3513.
[14] S.V. Stolyar, D.A. Balaev, V.P. Ladygina, A.A. Dubrovskiy, A.A. Krasikov, S.I. Popkov, et al., Bacterial ferrihydrite nanoparticles: preparation, magnetic properties, and application in medicine, J. Supercond. Nov. Magn. 31 (2018) 2297–2304, https://doi.org/10.1007/s10948-018-4700-1.
[15] K. Dobretsov, S. Stolyar, A. Lopatin, Magnetic nanoparticles: a new tool for antibiotic delivery to sinonasal tissues. results of preliminary studies, Acta Otorhinolaryngol. Ital. Organo Uff. Della Soc. Ital. Di Otorinolaringol. E Chir. Cerv. – Facc. 35 (2015) 97–102.
[16] S.A. Makhlouf, F.T. Parker, A.E. Berkowitz, Magnetic hysteresis anomalies in ferritin, Phys. Rev. B 55 (1997) R14717–R14720, https://doi.org/10.1103/PhysRevB.55.R14717.
[17] S.V. Stolyar, R.N. Yaroslavtsev, R.S. Iskhakov, O.A. Bayukov, D.A. Balaev, A.A. Dubrovskii, et al., Magnetic and resonance properties of ferrihydrite nanoparticles doped with cobalt, Phys. Solid State 59 (2017) 555–563, https://doi.org/10.1134/S1063783417030301.
[18] S.V. Stolyar, O.A. Bayukov, Y.L. Gurevich, E.A. Denisova, R.S. Iskhakov, V.P. Ladygina, et al., Iron-containing nanoparticles from microbial metabolism, Inorg. Mater. 42 (2006) 763–768, https://doi.org/10.1134/S0020168506070132.
[19] N.N. Golovnev, M.S. Molokeev, S.N. Vereshchagin, V.V. Atuchin, M.Y. Sidorenko, M.S. Dmitrushkov, Crystal structure and properties of the precursor [Ni(H2O)6](HTBA)2·2H2O and the complexes M(HTBA)2(H2O)2 (M=Ni Co, Fe), Polyhedron 70 (2014) 71–76, https://doi.org/10.1016/j.poly.2013.12.021.
[20] N.N. Golovnev, M.S. Molokeev, S.N. Vereshchagin, V.V. Atuchin, Calcium and strontium thiobarbiturates with discrete and polymeric structures, J. Coord. Chem. 66 (2013) 4119–4130, https://doi.org/10.1080/00958972.2013.860450.
[21] J.D. Russell, Infrared spectroscopy of ferrihydrite: evidence for the presence of structural hydroxyl groups, Clay Miner. 14 (1979) 109–114, https://doi.org/10.1180/claymin.1979.014.2.03.
[22] J.J. Powell, S.F.A. Bruggraber, N. Faria, L.K. Poots, N. Hondow, T.J. Pennycook, et al., A nano-disperse ferritin-core mimetic that efficiently corrects anemia without luminal iron redox activity, Nanomed. Nanotechnol. Biol. Med. 10 (2014) 1529–1538, https://doi.org/10.1016/j.nano.2013.12.011.
[23] M. Villacís García, M. Ugalde Arzate, K. Vaca Escobar, M. Villalobos, R. Zanella, N. Martínez Villegas, Laboratory synthesis of goethite and ferrihydrite of controlled particle sizes, Boletín La Soc. Geológica Mex. 67 (2015) 433–446, https://doi.org/10.18268/BSGM2015v67n3a7.
[24] L. Anghel, M. Balasoiu, L.A. Ishchenko, S.V. Stolyar, T.S. Kurkin, A.V. Rogachev, et al., Characterization of bio-synthesized nanoparticles produced by Klebsiella oxytoca, J. Phys. Conf. Ser. 351 (2012), https://doi.org/10.1088/1742-6596/351/1/012005 012005.
[25] L.J. Bellamy, The Infra-red Spectra of Complex Molecules, Springer, Netherlands, Dordrecht, 1975, http://doi.org/10.1007/978-94-011-6017-9.
[26] C. Pecharroman, T. Gonzalez-Carreno, J. Iglesias, The infrared dielectric properties of maghemite, γ-Fe2O3, from reflectance measurement on pressed powders, Phys. Chem. Miner. 22 (1995), https://doi.org/10.1007/BF00202677.
[27] R.K. Kukkadapu, J.M. Zachara, J.K. Fredrickson, S.C. Smith, A.C. Dohnalkova, C.K. Russell, Transformation of 2-line ferrihydrite to 6-line ferrihydrite under oxic and anoxic conditions, Am. Mineral. 88 (2003) 1903–1914.
[28] Y. Guyodo, S.K. Banerjee, R. Lee Penn, D. Burleson, T.S. Berquo, T. Seda, et al., Magnetic properties of synthetic six-line ferrihydrite nanoparticles, Phys. Earth Planet. Inter. 154 (2006) 222–233, https://doi.org/10.1016/j.pepi.2005.05.009.
[29] S.V. Stolyar, O.A. Bayukov, Y.L. Gurevich, R.S. Iskhakov, V.P. Ladygina, Mössbauer investigation of iron-producing bacteria Klebsiella oxytoca, Bull. Russ. Acad. Sci. Phys. 71 (2007) 1286–1290, https://doi.org/10.3103/S1062873807090201.
[30] A.P. Amulyavichus, I.P. Suzdalev, Investigation of the superparamagnetic properties of ultrafine iron particles by Mossbauer spectroscopy, JETP 37 (1973) 859.

Please cite this article as: S. V. Stolyar, O. A. Bayukov, R. N. Yaroslavtsev et al., Ion reduction in iron oxide and oxyhydroxide nanoparticles during ultrasonic treatment, Advanced Powder Technology, https://doi.org/10.1016/j.apt.2019.08.009